Journal of Nuclear Materials 392 (2009) 114–120

Contents lists available at ScienceDirect

Journal of Nuclear Materials

journal homepage: www.elsevier.com/locate/jnucmat

Self-diffusion near symmetrical tilt grain boundaries in UO_2 matrix: A molecular dynamics simulation study

E. Vincent-Aublant [a], J-M. Delaye [a], L. Van Brutzel [b,*]

[a] CEA, DEN, Sevice d'Étude et Comportement des Matériaux, F-30207 Bagnols-sur-Cèze, France
[b] CEA, DEN, Service de Chimie Physique, F-91191 Gif-Sur-Yvette, France

ARTICLE INFO

Article history:
Received 26 January 2009
Accepted 30 March 2009

PACS:
61.72.Mm
61.80.Lj
61.82.Rx

ABSTRACT

Molecular dynamics simulations have been carried out to study the influence of grain boundaries in stoichiometric UO_2 on uranium and oxygen self-diffusions over a large range of temperature varying from 300 K to 2100 K. The study was carried out on two symmetrical tilt grain boundaries, Σ5 and Σ41, which have respectively two different atomic structures. Firstly, the study of the temperature effect on the grain boundary core structure is presented. With the raise of temperature, the grain boundary core grows with an increase of disorder. Secondly, self-diffusion near both grain boundaries is studied. It has been found that grain boundaries accelerate the uranium and oxygen self-diffusion rates over several nanometres from the grain boundary interface. Uranium and oxygen self-diffusion are anisotropic, with a high acceleration along the grain boundary interface. Using the self-Van Hove correlation functions, hopping mechanisms were identified for Σ41 in all directions while for Σ5 hopping mechanism takes place along the grain boundary interface and random diffusion appears in the perpendicular direction of the grain boundary plane.

1. Introduction

After being in fission reactors during several years, spent nuclear fuel (uranium dioxide, UO_2) is put in storage condition. Under such conditions numerous self-radiations occur. Radiation activity combined with elevated temperatures at the beginning of the storage lead to alterations of the spent fuel's physical and mechanical properties. Among all the properties, self-diffusion is one of the most important phenomenon in the understanding and the characterization on the material evolution. Understanding the basic transport mechanisms at the atomic scale is crucial in the development of realistic macroscopic models. Moreover, grain boundaries (GBs) are known to amplify these changes, but their precise effects are not yet fully understood.

Uranium and oxygen self-diffusion was widely studied experimentally during the last 30 years in stoichiometric non-irradiated materials. These results have been reviewed in Refs. [1–4]. To determine the grain boundary effect, the results obtained in single crystals were generally compared to those obtained in polycrystalline materials. All these studies converged towards the same conclusions; GBs have no effect on oxygen self-diffusion, while uranium self-diffusion is largely accelerated in presence of grain boundaries. Recently, Sabioni et al. [5] carried out similar studies and in agreement with what was observed previously, they concluded that uranium self-diffusion in polycrystal, between 1771 K and 1970 K, is faster by five orders of magnitude than in single-crystal and that GBs, between 878 K and 1023 K, have no effect on oxygen self-diffusion. However, diffusion mechanisms are still unclear and approach at the atomic length scale with atomistic simulations can probe the basic transport phenomena as recently shown by Kupryazhkin et al. [6], which have compared oxygen and uranium self-diffusion mechanism at the surface, near-surface, and bulk in nanocrystal UO_2.

Molecular dynamics (MD) simulations with empirical interatomic potentials have been used with success to study the self-diffusion mechanisms occurring at the vicinity of GBs in metals [7–10] and other ceramics [11]. Herein, MD simulations were carried out to characterize the uranium and oxygen self-diffusions near symmetrical tilt GBs. In the first part of this paper, the effect of the temperature on the structure of two GBs (Σ5 and Σ41) is determined over a large range of temperature varying from 300 K to 2100 K. The second part is dedicated to the characterization of the uranium and oxygen self-diffusion. The distance until which the GB influences the self-diffusion is discussed. Then, the diffusion coefficients are calculated inside the GB core and compared to those calculated in the bulk. The last part discusses the diffusion mechanisms defined with self-Van Hove correlation functions.

2. Simulation method

The interatomic potential used for this study is the potential developed by Morelon et al. [12]. This potential has been compared with other available potentials by Govers et al. [13,14]. In this

* Corresponding author. Tel.: +33 1 69 08 79 15; fax: +33 1 69 08 92 21.
E-mail address: laurent.vanbrutzel@cea.fr (L. Van Brutzel).

0022-3115/$ - see front matter © 2009 Elsevier B.V. All rights reserved.
doi:10.1016/j.jnucmat.2009.03.059

study, Govers concluded that Morelon potential gives reliable structural properties and reproduces well the migration and formation energies of point defects, which is essential to study the diffusion. This potential is based on a Born–Mayer–Huggins-like potential for the repulsive part coupled with coulomb interaction. The analytical function of the potential is defined as:

$$V_{\alpha\beta}(r_{ij}) = A_{\alpha\beta}\exp\left(-\frac{r_{ij}}{B_{\alpha\beta}}\right) - \frac{C_{\alpha\beta}}{r_{ij}^6} + \frac{z_\alpha z_\beta}{4\pi\epsilon_0 r_{ij}}, \quad (1)$$

where A, B and C are adjustable parameters, r_{ij} is the distance between the atoms i and j, Z is the ionic partial charge and α and β refer to the type of atoms (herein either uranium or oxygen). Parameters and details on this potential can be found elsewhere [12].

A GB can be defined as an interface separating two single-crystals. Numerous different geometries can then be created. We have chosen to perform the study with symmetrical tilt GBs. The GB interface geometry can be characterized by five macroscopic degrees of freedom: the rotation axis of the crystal along the unit vector, $\vec{n}$, the misorientation angle, θ, between the two crystals and the three components of the normal vector, $\vec{n}_{GB}$, perpendicular to the interface plane. Fig. 1 represents a projection along the [001] tilt axis of a (310) symmetrical tilt boundary with a misorientation angle equal to $\theta = 36.87°$and noted: (310)/[001]Σ5. In the rest of the paper, the Cartesian axes (X,Y,Z) are defined as indicated in Fig. 1.

In our simulations, the interface created at the beginning of the simulation is constructed by specular inversion of a crystal rotated with an angle equal to $\theta/2$ on one half of the simulation box with respect to the interface plane. The periodic boundary conditions are used in the three directions. Consequently, two GB interfaces are created in the simulation box. For each temperature and each GB, relaxation is applied under NPT ensemble until the internal hydrostatic pressure reaches an average value below 0.1 GPa. The energies and the transport quantities were calculated and averaged after this relaxation phase.

Several symmetrical tilt GBs were previously studied at 300 K by MD simulation with the same interatomic potential [15]. It was found that for misorientation angles higher than 16° the GB structure is composed of Schottky defects whereas for misorientation angles lower than 16° the structure is composed of a line of edge dislocations. These two different structures involve different type of point defects. Therefore, self-diffusion has been studied, herein, near two different symmetrical tilt GBs representing both

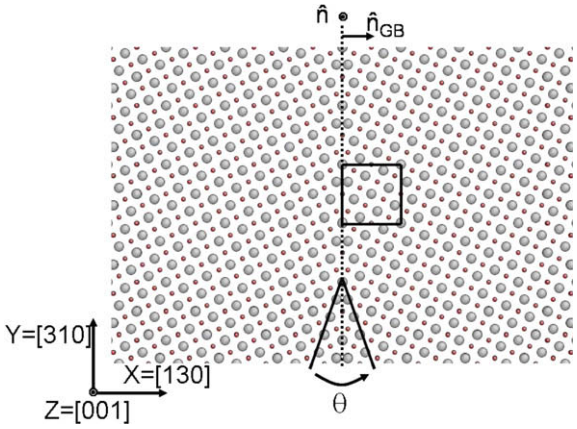

Fig. 1. Projection onto the [001] tilt direction of the symmetrical grain boundary (310)/[001]Σ5. The GB interface is underlined by the dashed line. The biggest spheres represent the uranium atoms and the smallest the oxygen atoms. The X axis is defined perpendicular to the GB interface and the Y and Z axes are parallel to the GB interface.

different structure types. We choose for the structure composed of edge dislocations the GB (910)/[001]Σ41, noted in the following as Σ41, with a misorientation angle of 12.8°, and for the structure composed of Schottky defects the GB (310)/[001]Σ5, noted in the following as Σ5, with a misorientation angle of 36.6°.

The self-diffusion coefficients are determined based on the time evolution of the uranium and oxygen mean square displacements (*msd*). This quantity can be easily determined by recording the atomic positions regularly during the simulation. The *msd* function at time t corresponds to the average square distance travelled by an atom between the time t_0 and the time t. It is calculated with the following equation:

$$msd(t) = \frac{1}{N}\sum_{i=1}^{N}\left[\vec{r}_i(t) - \vec{r}_i(t_0)\right]^2, \quad (2)$$

where N is the total number of ions (either uranium or oxygen), $\vec{r}_i(t_0)$ is the position of the atom i at the initial time, and $\vec{r}_i(t)$ the position at the time t. The self-diffusion coefficients, D, are deduced from the *msd* functions using the Einstein's relation:

$$D = \lim_{t\to\infty}\frac{1}{6t}msd(t). \quad (3)$$

Since infinite times are not accessible via MD simulations, the self-diffusion coefficients are extrapolated from the asymptotic slope of the *msd* functions.

In general, diffusion in solid occurs with point defects [16]. The point defect concentration is thermally activated, and it increases with the increase of temperature. Migration is also a thermally activated process, accelerated with increasing temperatures. The diffusion coefficient can then be written as follows:

$$D = D_0\exp\left(-\frac{E_f + E_m}{k_B T}\right), \quad (4)$$

where E_f is the formation energy of the point defect, E_m is the migration energy of the defect, D_0 is a pre-exponential factor independent of the temperature, k_B is the Boltzmann constant, and T the temperature. In certain cases, the crystal structure contains inherent concentration of point defects. For instance in hypo- or hyperstoichiometric matrices ($UO_{2\pm x}$) or in the GB core. In those cases, the point defect formation energy which regulates the point defects concentration is not included in the calculation of the diffusion activation energy. Only the migration energy is taken into account [17]. Thus, for GBs, the activation energy calculated from the slope of an Arrhénius diagram (log$D$ as a function of $1/k_BT$) is equivalent to the migration energy.

3. Results and discussion

3.1. Grain boundary core – temperature effect

At 300 K the Σ5 and the Σ41 core structures are different. When the temperature increases, both core structures become more disordered due to the thermal vibrations. It is then difficult to distinguish differences. To illustrate this evolution, the total pair correlation functions, noted $g(r)$, is calculated from the following equation:

$$g(r) = \frac{V}{N}\left\langle\sum_{i=1}^{N}\sum_{j\neq i}^{N}\delta(r - r_{ij})\right\rangle, \quad (5)$$

where N is the total number of atoms, V the volume of the simulation box, and r_{ij} the distance between the atoms i and j. The brackets denote a statistical average over different configurations. The $g(r)$ functions are only calculated for atoms included in a 0.5 nm slab around the GB interfaces at 300 K and 1500 K. Thus, only the GB

core structure is investigated. The results are plotted in Fig. 2. Differences are noticeable at 300 K and indicate the dissimilarity of both GB core structures. At 1500 K, both $g(r)$ functions are comparable and both structures seem identical. However, they are more disordered since less peaks are well defined.

Because the potential energy per atom depends on its local environment, an alternative to measure the temperature influence on GB core structures, is to calculate the evolution of the potential energy per atom with temperature. With our potential the average potential energy of an uranium atom in the bulk at 300 K is equal to −7.9 eV and of an oxygen atom to −2.2 eV. In order to calculate the evolution of the average potential energy per atom in the vicinity of a GB, slabs of 0.02 nm width along the X axis (perpendicular to the GB) are defined. The average potential energies per atom are then calculated in each slab for both GBs and for temperatures ranging from 300 K to 2100 K. Fig. 3 represents the evolution of the uranium and the oxygen potential energies versus the distance from the Σ5 GB interface. Similar results are found for Σ41. For each temperature, the average potential energy obtained in the bulk (straight lines) is added for comparison.

For all temperatures, we observe a big peak at the interface with high potential energies. This peak is followed by a region where the potential energy is almost constant and close to the average potential energy calculated in the bulk. Therefore, one can define the region of influence of the GB as the region where the potential energy is greater than the average potential energy of the bulk (i.e. length from the interface to the distance at which the potential energy is equal to the average potential energy of the bulk). The high value of the potential energy is due to the presence of numerous point defects at the interface and to the elastic deformation of the UO_2 lattice. The size of this region increases with the temperature. At 300 K, the Σ5's width equals about 2 nm, and it increases to about 5 nm at 1500 K to reach more than 8 nm at 2100 K. However, at high temperatures (higher than 1500 K) oscillations appear between GBs, especially in the oxygen sub-lattice. We hypothesize that this is due to structural instabilities, which arise from elastic interactions between both GBs.

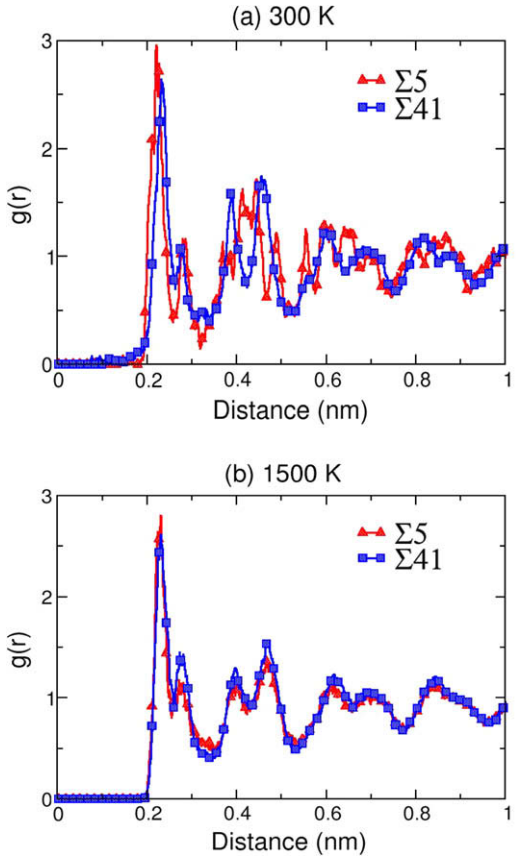

Fig. 2. Plots of the total pair correlation functions, $g(r)$, calculated in the vicinity of the GBs Σ5 and Σ41 at: (a) 300 K and, (b) 1500 K.

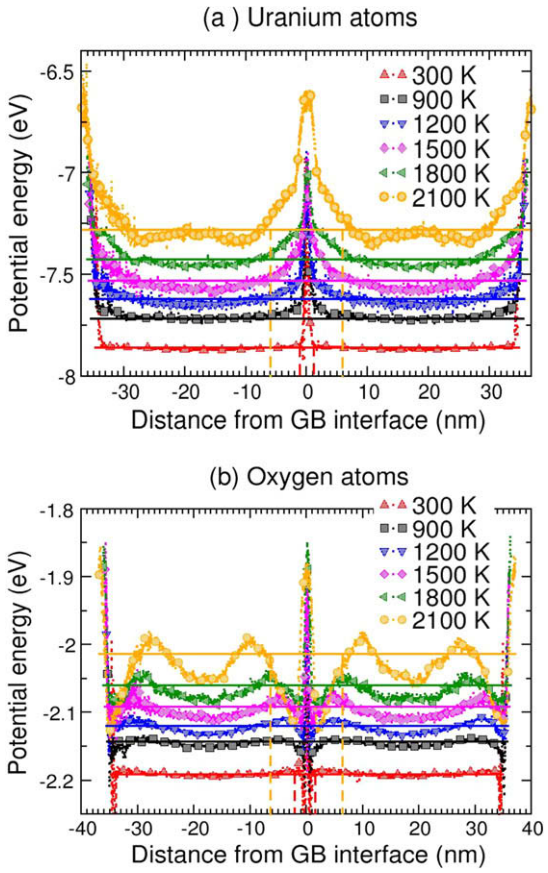

Fig. 3. Plots of the evolution of the average uranium (a) and oxygen (b) potential energies with the distance from the Σ5 GB interface. Slabs of 0.02 nm width are used to calculated the average potential energies. The straight lines are the average potential energies per atom obtained in bulk for temperatures ranging from 300 K to 2100 K.

3.2. Self-diffusion coefficients

3.2.1. Self-diffusion coefficient evolution with the distance from the grain boundary

To study the influence of GB on self-diffusion coefficients the simulation box was divided into 0.3 nm width slabs along the X axis parallel to the GB plane. Self-diffusion coefficients were calculated with the *msd* functions, Eq. (3), for the atoms in each slab at the beginning of the relaxation phase. Fig. 4 shows the evolution of the oxygen self-diffusion coefficients at 1500 K for Σ5 and Σ41 as a function of the distance from the GB interface in the region of influence of the GB found in the previous Section 3.1 (5 nm). They are compared with the bulk oxygen self-diffusion coefficient, obtained previously in UO_2 single-crystal [18].

Both grain boundaries have similar influence on the oxygen self-diffusion behaviour. Three distinct regions can be distinguished, separated in Fig. 4 with dashed vertical straight lines. In the first region, which corresponds to what we call the GB core, the self-diffusion coefficient is maximum. This region is narrow and measures, for this temperature, approximately 0.6 nm width from the interface. A second region, where diffusion coefficients

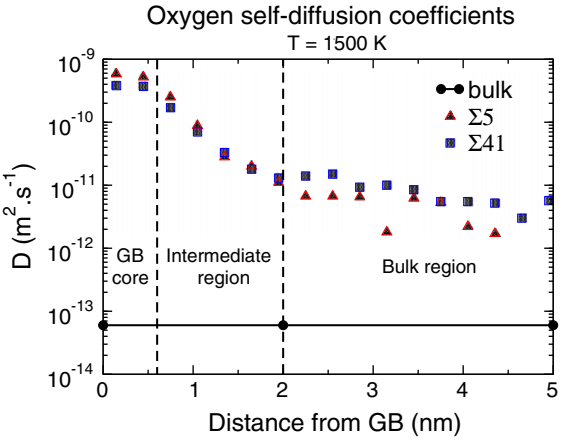

Fig. 4. Plots of the oxygen self-diffusion coefficients as a function of the distance from the interface. They are calculated per slabs of 0.3 nm width parallel to the GB plane. The average oxygen self-diffusion coefficient calculated in the bulk at 1500 K is also plotted.

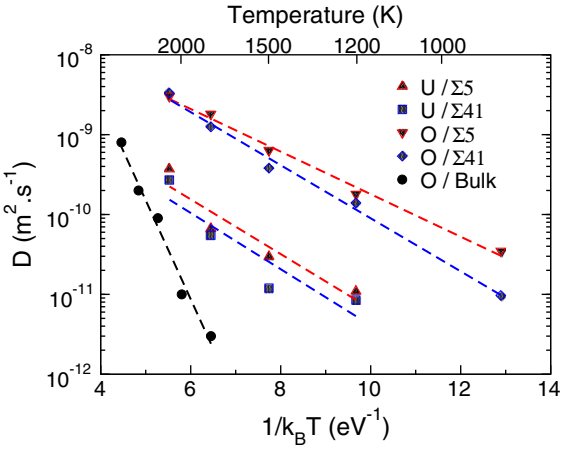

Fig. 5. Uranium and oxygen self-diffusion coefficients as a function of $1/k_BT$ calculated for atoms included in Σ5 and Σ41 GB cores.

decrease gradually, extends until a distance equal to about 2 nm. It is referred to the intermediate region. In this region, the self-diffusion coefficients decrease by more than one order of magnitude. In the last region, the diffusion coefficients are slightly decreasing. Nevertheless, each self-diffusion coefficient is still two orders of magnitude higher than those calculated in the bulk at a distance of 5 nm from the interface. The required distance at which the value of the self-diffusion coefficient will reach the value of the self-diffusion coefficient in the bulk is hardly extrapolable with our simulations. However, it should be at least in the order of several tens nanometres. It seems that the GB has a large influence, whatever its structure, on the oxygen self-diffusion in UO_2.

Uranium self-diffusion coefficients are much smaller than the oxygen self-diffusion coefficients. In the bulk, due to the time limit of the MD simulation, we were not able to calculate any uranium self-diffusion. However, we were able to measure them at 1200 K, but for a distance lower than 1.2 nm from the GB interface. Until a distance of 0.6 nm, the self-diffusion coefficients are on the order of 10^{-10} m^2 s^{-1}. Then, they decrease rapidly to reach about 10^{-13} m^2 s^{-1} at a distance of 1.2 nm. Therefore, GB seems to influence as well the uranium self-diffusion.

3.2.2. Self-diffusion coefficient evolution with temperature

In order to study the diffusion at the GB, we calculate the evolution of self-diffusion coefficients as a function of the temperature in the region of the GB core defined in the above Section 3.2.1. The calculation was carried out in Σ5 and Σ41 from temperatures ranging from 900 K to 2100 K. The results are presented in Fig. 5 in an Arrhénius representation (i.e. log$D$ as a function of $1/k_BT$, where k_B is the Boltzmann constant). For comparison, the evolution of the oxygen self-diffusion coefficients calculated in the bulk is also represented in the same graph. The evolution of the uranium self-diffusion coefficients in the bulk is not plotted because they are too small to be calculated with MD simulations in a reasonable amount of time.

The graphs clearly show that oxygen self-diffusion is much faster than the uranium self-diffusion. This behaviour is similar to the one observed in single-crystals [1,2]. However, self-diffusion coefficients are higher at the GBs than in the bulk. Indeed, for the uranium atoms, it is possible to calculate self-diffusion coefficients from temperatures higher than 1200 K. This result indicates that self-diffusion is accelerated in the GB core. This is not surprising considering the high number of point defects present in the GB core.

Table 1
Activation energies (E_a) and pre-factors (D_0) resulting from the fit of the Arrhénius diagram.

	U Σ5	U Σ41	O Σ5	O Σ41	O Bulk
D_0 (m^2 s^{-1})	1.8×10^{-8}	1.4×10^{-8}	8.3×10^{-8}	1.9×10^{-7}	4.16×10^{-4}
E_a (eV)	0.79	0.81	0.61	0.77	2.94

The values of the activation energies as well as the values of the pre-factors resulting from the fit of the data with the Eq. (4) are gathered in Table 1. As explained in Section 2, the activation energy is equal to the migration energies when the intrinsic defect concentration is much higher than the thermally activated defect concentration.

The uranium migration energies obtained near the GBs are low, about 0.8 eV. This value is much lower than the point defect migration energies calculated in the bulk with *ab initio* simulations by Durinck et al. [19] (4.4 eV for the vacancy migration and 5.8 eV for the interstitial), and lower than the activation energy measured experimentally in polycrystalline UO_2 matrices (3.03–4.68 eV [20]). This result confirms that GB considerably facilitates the migration of uranium atoms. This is in agreement with recent experiments carried out by Sabioni et al. [4] who measured an increase of five orders of magnitude for the uranium self-diffusion coefficient near a GB compared with the one in a single-crystal.

The oxygen migration energies are twice smaller than those calculated via *ab initio* by Durinck for vacancy mechanism (E_m = 1.2 eV) or interstitial mechanism (E_m = 1.1 eV) in stoichiometric UO_2. Nevertheless, they are close to the activation energies measured experimentally in hyper-stoichiometric matrices (E_a = 0.91 eV) [20]. Like in GBs, the introduction of vacancies or interstitials in hypo- or hyper-stoichiometric compounds accelerates considerably the oxygen self-diffusion. However, no acceleration of the oxygen self-diffusion has been observed experimentally for polycrystalline UO_2 compared to single-crystals [1,5], which is in disagreement with the present calculations. The discrepancy could be due to the difficulty to maintain perfect stoichiometric ratio during the measurements, which would accelerate the oxygen self-diffusion. It could be due also to the fact that our calculation are concentrated on particular symmetrical GBs and other calculations on different GB structure are desirable.

Comparison of pre-factors has to be considered herein with caution because self-diffusion is accelerated with pre-existing defects. The pre-factor is then proportional to the intrinsic defect concentration, which is a function of the stoichiometry. It will be necessary to

know the defect concentration in all the different matrices to be able to interpret the difference between the pre-factors. However, it is difficult to determine the defect concentration in the GB core because of the relaxation and of the arbitrary choice of the GB core width in which self-diffusion coefficients are calculated.

For the oxygen atoms, the migration energy obtained for Σ5 is smaller than those determined for Σ41 indicating that oxygen migration is easier in Σ5. The difference stems certainly from the difference of structure between both GBs. However, at high temperature both self-diffusion coefficients are almost identical which could be explained by the similarity of both GB structures demonstrates in Section 3.1. For the uranium atoms, the migration energy and the pre-exponential factor are very similar for both GBs, indicating that their diffusion may not be influenced much by the GB structure.

3.3. Self-diffusion mechanism

To determine the main direction of diffusion, mean square displacements were calculated separately along each of the three directions; *X*, *Y*, and *Z*. Because we focus on the self-diffusion at the GB, we consider only atoms included in the GB core region. The time evolution of these mean square displacements calculated at 1500 K are reported in Fig. 6 for both Σ5 and Σ41 and both uranium and oxygen atoms. Similar results, not represented herein, are obtained at different temperatures.

For both GBs, mean square displacements in all directions increase linearly with time after a relaxation period of approximately 10 ps. However, in all the cases, the slopes of the curves obtained in the *X* direction are smaller than for the other directions (*X* corresponds to the direction perpendicular to the GB plane). This indicates that self-diffusion is anisotropic and higher along the grain boundary plane (*YZ*), whatever the structure or the type of ion. This result is not surprising because more point defects are sitting along the interface, which accelerates the diffusion.

To further investigate the diffusion mechanism near the GB, the self-part of the Van Hove space-time autocorrelation functions [21] were calculated. The Van Hove autocorrelation function highlights the dynamical correlations of the atom trajectories. It is then possible to evaluate if the diffusion is either an hopping process or not (Brownian motion). The self-part Van Hove function, noted $G_{self}(\vec{r},t)$, is defined by the following relation:

$$G_{self}(\vec{r},t) = \frac{1}{N}\left\langle \sum_{i=1}^{N} \delta[\vec{r} + \vec{r}_i(0) - \vec{r}_i(t)] \right\rangle, \tag{6}$$

where N is the number of either uranium or oxygen atoms, $\vec{r}_i(0)$ corresponds to the initial position of the atom i and $\vec{r}r_i(t)$ corresponds to the position of the atom i at the time t. The brackets denote a statistical average over different configurations. With this definition, $G_{self}(\vec{r},t)$ gives the probability that within time t a particle moves by $\vec{r}$. The $G_{self}(\vec{r},t)$ functions were determined for both Σ5 and Σ41 at 1500 K for atoms included in the GB core region. For the spatial discretization an increment of 10^{-2} nm is used. The results of these $G_{self}(\vec{r},t)$ functions are plotted in Figs. 7 and 8 for uranium and oxygen atoms respectively, for four consecutive time intervals (0.045 ps (a), 0.45 ps (b), 0.96 ps (c), and >200 ps (d)). The functions were not normalized with respect to the total number of atoms in order to obtain different intensities, which allows better visualization.

For the short time intervals (Figs. 7(a) and 8(a)), only one peak appears at about 0.05 nm for each case. This is due to thermal vibrations where atoms oscillate around their initial positions. For longer time intervals, several distinct peaks appear at the same well defined distances in both GBs. This clearly indicates a hopping process, and reveals that a subjacent ordered structure does exist for both GBs. However, differences appear between the uranium and the oxygen sub-lattices. Only one small peak appears for the uranium atoms at about 0.39 nm, corresponding to the distance of the first uranium–uranium nearest neighbour. Whereas, for the oxygen atoms at least four peaks identified to the successive nearest neighbours oxygen–oxygen are defined until a distance of 0.85 nm. Furthermore, the intensities of the 2nd, 3rd, and 4th peaks are higher than the intensity of the first one indicating that most of the oxygen atoms have moved from their original position.

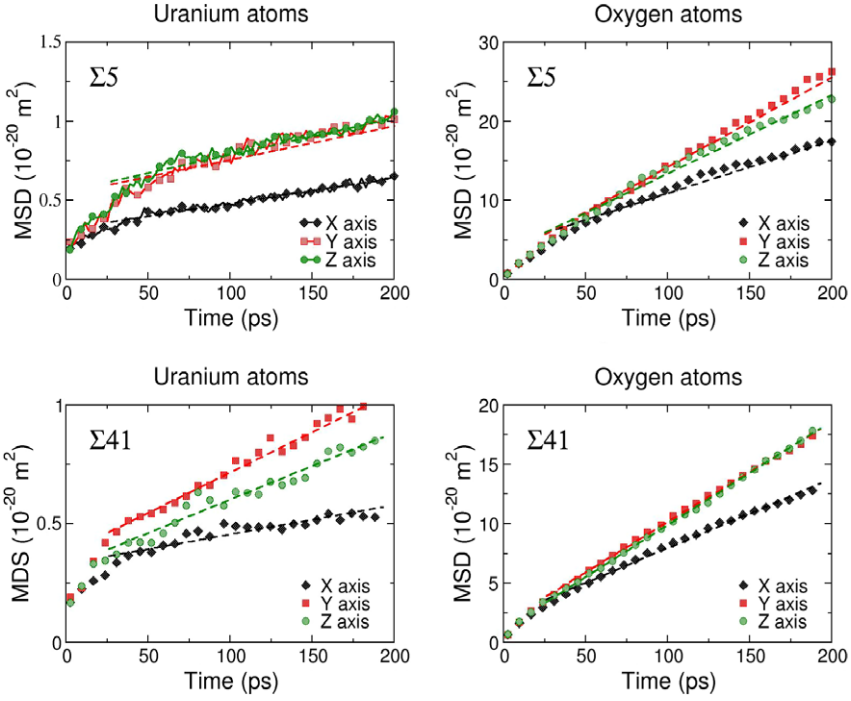

Fig. 6. Mean square displacements along the *X*, *Y*, and *Z* axes as a function of time calculated at 1500 K for both uranium and oxygen atoms in Σ5 and Σ41 GBs.

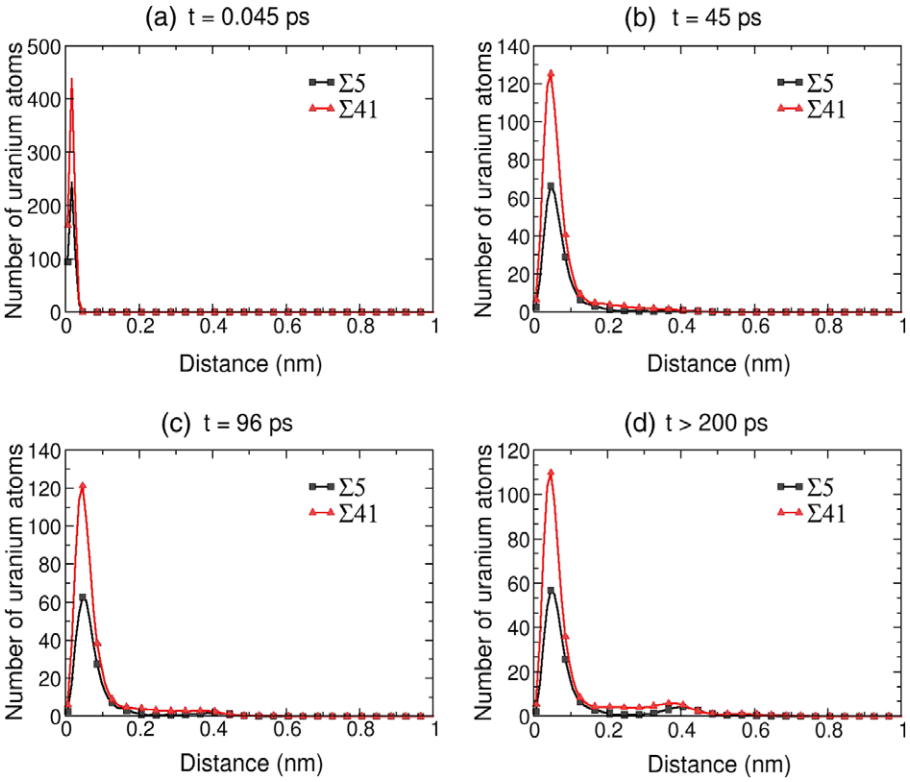

Fig. 7. Self-Van Hove functions for uranium atoms for Σ5 and Σ41 at different time intervals.

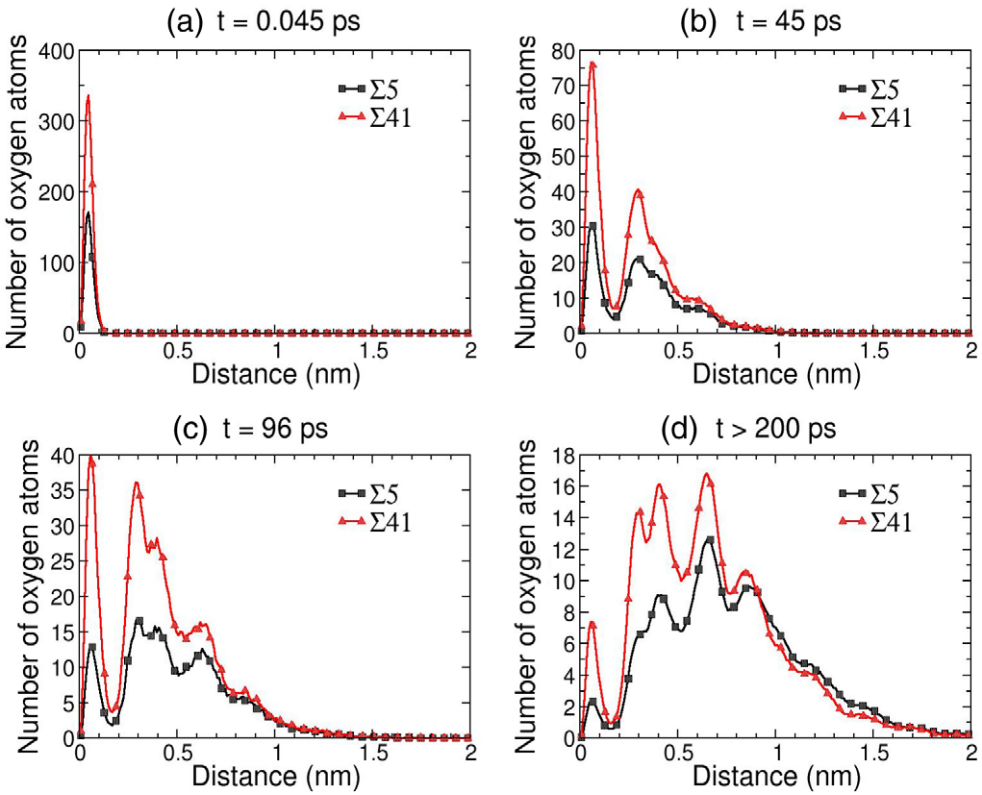

Fig. 8. Self-Van Hove functions for oxygen atoms for Σ5 and Σ41 at different time intervals.

In order to better characterize the anisotropy of the self-diffusion near the GB, the self-Van Hove functions has been calculated separately for the *X* axis only and for the *Y* and *Z* axes. These two partial functions are defined as follows:

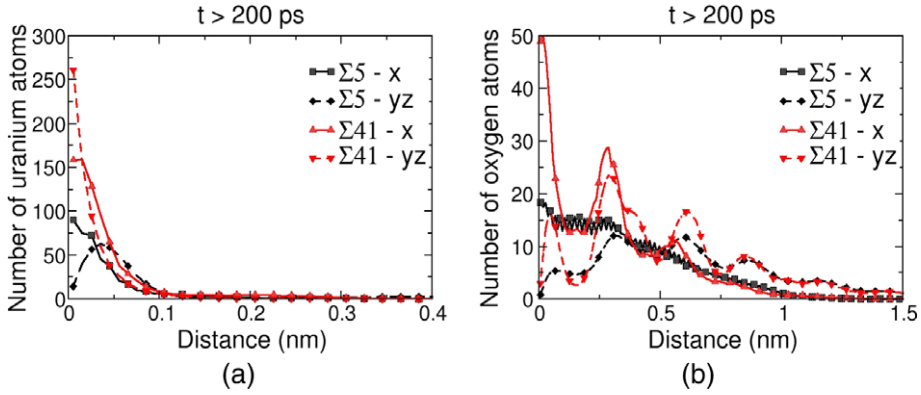

Fig. 9. Partial self-Van Hove functions for uranium (a) and oxygen (b) atoms near Σ5 and Σ41 GBs calculated for a time interval superior to 200 ps.

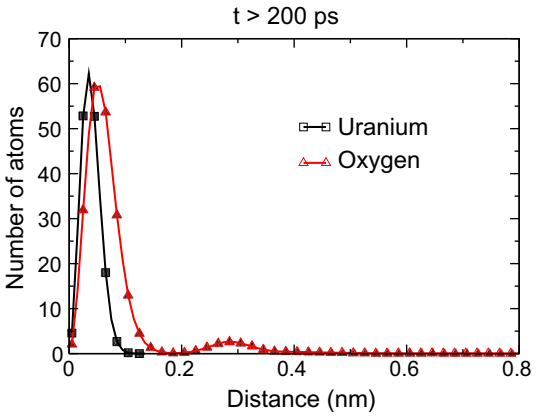

Fig. 10. Self-Van Hove functions for uranium and oxygen atoms in the bulk calculated for a time interval superior to 200 ps.

$$G_{self}(x,t) = \frac{1}{N}\left\langle \sum_{i=1}^{N} \delta[x + x_i(0) - x_i(t)] \right\rangle, \quad (7)$$

$$G_{self}(\vec{r}_{yz},t) = \frac{1}{N}\left\langle \sum_{i=1}^{N} \delta[\vec{r}_{yz} + \vec{r}_{iyz}(0) - \vec{r}_{iyz}(t)] \right\rangle, \quad (8)$$

where $\vec{r}_{yz}$ represents a position vector defined by only the Y and Z atom coordinates. These functions have been calculated, in both GBs, for atoms included in the GB core region and for atoms included in the bulk, which is considered as a region without point defects. Fig. 9(a) and (b) plot the results of these functions for a time interval greater than 200 ps.

For the uranium atoms, the peaks are hardly distinguishable due to the small self-diffusion. Nevertheless, it seems that there is no noticeable discrepancy between the different axes for both GBs. For the oxygen atoms, different behaviours appears clearly between the *X* axis in one hand and the *Y* and *Z* axes on the other hand in the case of the GB Σ5. For this GB, all the peaks defined previously, for the *Y* and *Z* axes, appear while the function decreases stately for the *X* axis. The hopping process takes place only along the interface plane (*YZ*) while along the axis, perpendicular to the interface (*X* axis), self-diffusion is rather random. For the GB Σ41, both functions show peaks centred at the same distances. Thus, the lattice sites used for the hopping oxygen self-diffusion process, in this type of GB, are ordered in a 3D space.

Finally, in order to compare with the self-diffusion mechanism in the bulk, the self-Van Hove functions have been calculated in the bulk at 1500 K for both uranium and oxygen atoms and are represented in Fig. 10. The uranium self-diffusion is undetectable while only one peak at a distance corresponding to the first oxygen–oxygen nearest neighbour (0.287 nm) appears slightly. The oxygen self-diffusion is then significantly slower than in the GB core region. This result is coherent with the self-diffusion coefficients calculated in Section 3.2.2. However, the same hopping mechanism is taking place.

3.4. Conclusion

Molecular dynamics simulations with empirical potential have been carried out to study uranium and oxygen self-diffusion near symmetrical tilt grain boundaries Σ5 and Σ41. First, it has been observed an acceleration of the diffusion near GB for both uranium and oxygen atoms. For the highest values of the self-diffusion coefficients, we defined the GB core, which is about one nanometre thick. Nevertheless, the influence on the diffusion of the GB continues over several tenths of nanometres. This acceleration is certainly due to the presence of point defects along the GB interfaces. In both GBs, diffusion has been found to be anisotropic. The diffusion is greater along the GB interface than perpendicular to the GB plane. Moreover, with the analysis of the partial-Van Hove functions, two different mechanisms for the oxygen atoms have been found. In Σ41 oxygen diffusion occurs with hopping mechanisms in 3D, whereas in Σ5, we observed a hopping mechanism along the GB interface and a random diffusion in the direction perpendicular to the interface.

References

[1] J. Marin, P. Contamin, J. Nucl. Mater. 30 (1969) 16.
[2] J. Belle, J. Nucl. Mater. 30 (1969) 3.
[3] H. Matzke, J. Chem. Soc. Faraday Trans. II 83 (1987) 1121.
[4] A. Sabioni, W. Ferraz, F. Millot, J. Nucl. Mater. 257 (1998) 180.
[5] A. Sabioni, W. Ferraz, F. Millot, J. Nucl. Mater. 278 (2000) 364.
[6] A. Kupryazhkin, A. Zhiganov, D. Risovany, K. Nekrassov, V. Risovany, V. Golovanov, J. Nucl. Mater. 372 (2008) 233.
[7] T. Kwok, P. Ho, S. Yip, Phys. Rev. B 29 (1984) 5363.
[8] P. Keblinski, D. Wolf, S. Phillpot, Philos. Mag. A 79 (1999) 2735.
[9] B. De Bas, D. Farkas, Intermetallics 12 (2004) 937.
[10] A. Suzuki, Y. Mishin, J. Mater. Sci. 40 (2005) 3155.
[11] C. Fisher, H. Matsubara, Comput. Mater. Sci. 14 (1999) 177.
[12] D. Morelon, N.D. Ghaleb, J. Delaye, L. Van Brutzel, Philos. Mag. 83 (2003) 1533–1550.
[13] K. Govers, S. Lemehov, M. Hou, J. Nucl. Mater. 366 (2007) 161.
[14] K. Govers, S. Lemehov, M. Hou, J. Nucl. Mater. 376 (2008) 66.
[15] L. Van Brutzel, E. Vincent-Aublant, J. Nucl. Mater. 377 (2008) 522.
[16] C. Flynn, Point Defects and Diffusion, Clarendon, 1972.
[17] A. Auskern, J. Belle, J. Nucl. Mater. 3 (1961) 267.
[18] L. Van Brutzel, A. Chartier, J. Crocombette, Phys. Rev. B 78 (2008) 024111.
[19] J. Durinck, M. Freyss, P. Garcia, Atomic transport simulations in UO_{2+x} by ab-initio: oxygen and uranium atomic migration, Tech. Report, Internal Report CEA-SESC/LCC 07-009, 2007.
[20] P. Contamin, J. Bacmann, J. Marin, J. Nucl. Mater. 42 (1972) 54.
[21] L. Van Hove, Phys. Rev. 95 (1954) 249.